

Regular Paper

Performance Evaluation of Synchronous Variable-multiple Collision Avoidance Systems

HIROSHI KOBAYASHI^{1,a)} KAORU SANO² OSAMU MORIYA³

Received: June 20, 2014, Accepted: December 3, 2014

Abstract: To address the digital divide in developing countries, fixed wireless access (FWA) networks have the potential to quickly provide economical access over a wide area within a radius of tens of kilometers. The conventional synchronous variable-multiple collision avoidance (v-MCA) system, which is referred to as a non-precedence (NP) system, can be operated over a network of any size without the need to use frame-length restrictions. However, it has a potential drawback of rapid degradation of the throughput due to the intervention of the round trip time, which is proportional to the network length and upload bandwidth. The advanced synchronous v-MCA system incorporating total precedence (TP) transmission of frames provides high throughput regardless of network length and upload bandwidth. In this paper, after showing the medium access control mechanisms of the NP and TP systems, their theoretical calculation models are discussed in detail. Then, their system performances are evaluated and overlooked by comparing theoretical and simulated results. The TP system provides an ultimate maximum throughput performance regardless of network length and total upload bandwidth, while maintaining the low delay characteristics of a contention-based access scheme.

Keywords: synchronous v-MCA, split channel MAC, broadband access network, point to multipoint, out-of-band signaling

1. Introduction

Broadband Internet access has been popularized primarily in developed countries. The construction of access networks for solving the digital divide in developing countries will be an important issue in the near future. As shown in **Fig. 1**, the use of fixed wireless access (FWA) media, such as the 2–11 GHz licensed frequency band, is a potential solution to providing economical high-speed access over a wide area within a radius of tens of kilometers.

The data-over-cable service interface specification (DOCSIS), which was originally developed for hybrid-fiber-coaxial

(CATV/HFC) systems, was adapted for use in systems that are based on the Worldwide Interoperability for Microwave Access (WiMAX). However, the access control procedure of DOCSIS is conducted in a reservation (Request-and-Grant) cycle in the order of 2–4 msec. The potential drawback of this approach is that the acknowledgments in TCP communications must also go through the Request-and-Grant cycle, i.e., this approach hampers downstream throughput in applications that require fast communication times, such as online games. However, it is suitable for applications that use connection-oriented traffic, such as real-time audio, streaming video, or large file transfers, in which packets can be sent consecutively according to an increasing the window size [1], [2], [3].

The conventional synchronous variable multiple collision avoidance (v-MCA) system, which is referred to as the NP (non-precedence) system, is a contention-based access (CBA) system. To reduce the probability of collisions, the number of variable collision avoidance (CA) slots is controlled adaptively based on the volume of traffic. It can be operated over a network of any length without the use of frame-length restrictions because the colliding frames encounter collisions from their first bits. However, a potential drawback of rapid degradation of the throughput due to the round trip time (*RTT*) for a more exact round trip bit-time, which is proportional not only to the network length but also to the upload bandwidth [4], [5], [6].

The advanced synchronous v-MCA system incorporates the total precedence transmission of frames and is referred to as the TP system. This system aims to precede the transmission of CA and medium access control (MAC) frames to determine the time of

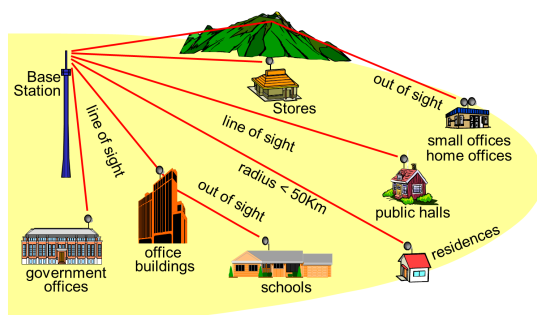


Fig. 1 An image of fixed wireless access networks.

¹ The Graduate School of Advanced Science and Technology, Tokyo Denki University, Inzai, Chiba 270–1382, Japan

² The School of Information Environment, Tokyo Denki University, Inzai, Chiba 270–1382, Japan

³ Social Infrastructure Systems Company, TOSHIBA CORPORATION, Kawasaki, Kanagawa 212–8581, Japan

^{a)} hirokoba@mail.dendai.ac.jp

carrier-signal extinction when the base station (BS) has just received CA or MAC frames and to minimize the time lost for upload channels due to the intervention of RTT . Thus, the TP system is expected to achieve an ideal performance regardless of the network length and total upload bandwidth, and it should maintain the low-delay characteristic of CBA control [7], [8], [9].

However, these existing studies make comparisons regarding the NP and TP systems. They used simulations between the maximum throughput for offered traffic changes under several network conditions and changes in delay in such a situation after showing the theoretical equations of the maximum throughput of the TP system. Thus, it has been difficult to understand the maximum throughput for the changes in network conditions and delay in such a situation, i.e., the system characteristics in the whole applicable domain of the system.

This study has revealed the system characteristics for the whole applicable domain of the system after showing the theoretical equations of the maximum throughput and the delay characteristics regarding both the NP and TP systems.

In this paper, first, the MAC mechanisms of the NP and TP systems are described. Next, their theoretical calculation models are discussed in detail. Finally, system performances within the target range are evaluated by making a comparison between theoretical and simulated results.

2. Medium Access Control Mechanisms

2.1 NP System

On point-to-multipoint (PTMP) networks that generally consist of different upload and download frequency bands, media access control is necessary to limit contention with user MAC frames sent from customer premises equipment (CPEs) with directional antennas to a BS. On the other hand, only the BS transmits user MAC frames to CPEs without contention. Therefore, this study focuses on MAC for uploads.

The sharing transmission medium of a BS and several fixed CPEs has a feature that is absent in most LANs, such as Ethernet and wireless LAN, which work on the basis of equally distributed control. In the equally distributed access method, i.e., in almost all of the contention-based MAC schemes such as CSMA, CSMA/CD, CSMA/CA, and split-channel MAC, each device has the responsibility of executing its own carrier-sense or collision detection functions [4], [5], [6], [7], [8], [9]. Thus, these conventional schemes have been adopted for limited service area networks, such as LANs, to effectively manage their throughput performance.

Because all frames sent from CPEs reach the BS in fixed wireless PTMP networks, the BS can precisely control the signal level and the transmission timing of upload frames, as will be described later. Thus, the BS can provide functions corresponding to carrier-sense and collision detection on behalf of CPEs^{*1} [4], [5], [6].

The NP system that uses these features consists of the follow-

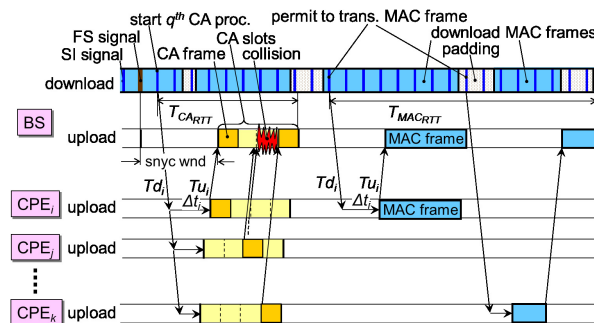


Fig. 2 An implementation of the NP system.

ing steps, as shown in Fig. 2:

- (A) The download signal is transmitted continuously without interruption. It consists of the periodic frame synchronization (FS) signal (e.g., 5.12 ms), the periodic status indication (SI) signals (e.g., 25.6 μ s), download MAC frames containing the user payloads, and the padding frames, as shown in Fig. 2.
- (B) The arrival of uploaded frames to the BS is forced to be equal to the signal level and is also forced to be synchronized with the bit and frame timing.
- (C) The BS sets n , the number of CA slots to be prepared during the next CA procedure, based on the estimated number of CPEs that attempt the current CA procedure; next, the BS advertises the permissions for CA frame transmission through the SI signal (“start q^{th} CA proc.” in Fig. 2).
- (D) CPEs, which have MAC frames to be transmitted, choose one of the advertised CA slots randomly and send the CA frames, which consist of random data and an error check code for collision detection, the length of the MAC frame to be transmitted and guard-bits between adjacent CA frames (“CA frame” in Fig. 2).
- (E) The BS checks whether an error is detected in the received CA frames, i.e., it picks up the CPEs that have succeeded in the CA procedure. Then, the BS transmits the SI signals as the bit-pattern (“1001” for CPE_{*i*} and “0001” for CPE_{*k*} in the case of Fig. 2^{*2}) to indicate MAC frame transmission to the CPEs.
- (F) After completing all MAC frame transmissions, the BS activates the next CA procedure by returning to Step (C).
- (G) CPEs, if unsuccessful in the CA procedure (“collision” by CPE_{*j*} and others that sent CA frames to the third CA slot in Fig. 2) through the bit pattern, retry the CA procedure again after the CA slot-based binary exponential back-off (BEB) processing with the delay based on the number of CA attempts before a successful CA procedure is achieved.

Steps (A) and (B) form the basis of synchronization and control in the entire system. The propagation delays for the download and upload (T_{d_i} and T_{u_i} in Fig. 2) are measured by inserting the synchronization window (“sync wnd” in Fig. 2) in the upload just after the FS signal. The sequence is as follows (not shown in

^{*1} “CSMA” was added to the scheme name such as CSMA/v-MCA in previous studies [4], [5], [6], [7], [8], [9], [10]. However, “v-MCA,” which excludes CSMA, is used in this paper, because no carrier-sense function is actually mounted in the system.

^{*2} When the BS advertises “1001,” which indicates that the two CPEs have succeeded in the CA procedure, the CPE_{*i*}, which transmitted the CA frame to the first CA slot, will then transmit the MAC frame. When the BS receives this, it will then advertise “0001.” Following this, CPE_{*k*}, which transmits the CA frame to the fourth CA slot, will transmit the MAC frame.

Fig. 2): The BS transmits the access synchronization (AS_i) signal to CPE_i . The CPE_i that received the AS_i signal immediately returns the response signal (RS_i) to the BS, which calculates the transmission timing to be adjusted at CPE_i (Δt_i in Fig. 2) by subtracting the interval between the time of sending AS_i and the time of receiving RS_i , i.e., $Td_i + Tu_i$ from T_{RTT} , where T_{RTT} is RTT , which covers the network length from the BS to the farthest CPE and includes the time for bit and frame synchronizations.

The signal level to be adjusted at CPE_i is also measured using RS_i , so that the level of the received RS_i becomes equal to the specific signal level at the BS. The transmission timing and the signal level to be adjusted are measured in order and advertised periodically (e.g., every 5 seconds) to the corresponding CPE by the BS. Thus, collision at the CA slots can be firmly detected regardless of network length, because the colliding CA frames encounter collisions from their first bits. The system name of “synchronous” v-MCA is derived from this synchronization scheme.

Steps (C) to (F) show the sequence of the CA procedure and the MAC frame transmission procedure, where the calculation of the number of variable CA slots n will be described later.

In Step (G), CPE, which has been informed of its collision occurrence in the CA procedure, does not attempt to retransmit immediately in order to reduce the probability of repeat collision occurrences by using the BEB algorithm that will be explained later.

For the conventional CSMA/CA system used on wireless LANs, the CA procedures are managed by the terminals. Only one MAC frame can be sent by a CA procedure [14]. On the other hand, in the NP system, the dispersion of the access, i.e., the reduction of collision occurrence probability in the CA procedure, is implemented by controlling the number of CA slots based on the offered traffic. As a result, low delay is achieved because the CA procedure time decreases due to the low number of CA slots in low offered traffic, while a high throughput is achieved because the success of the CA procedure is high as a result of many CA slots being prepared for high offered traffic.

However, in the NP system, the RTT intervenes between the BS and CPE every time when signaling a CA procedure and MAC frame transmission. Therefore, the throughput performance degrades rapidly due to the intervention of two RTT s, which depend on the longer network length and the wider upload bandwidth. A solution to eliminate this intervention is the TP system described below.

2.2 TP System

The intervention of the two RTT s is caused by Steps (C) to (F) or namely it is caused by the so-called in-band signaling (IBS) in which transmission for both the access control and the MAC frame uses the same frequency band [12], [13], [14], [15], [16]. IBS was used in the former analog telephone network, but out-of-band signaling (OBS) was introduced in digital telephone networks, such as ISDN, in which various new signaling services became feasible.

When introducing OBS with total precedence transmission of frames into the system, to enable the CA procedure and MAC frame transmission to run independently, all CA and MAC frames

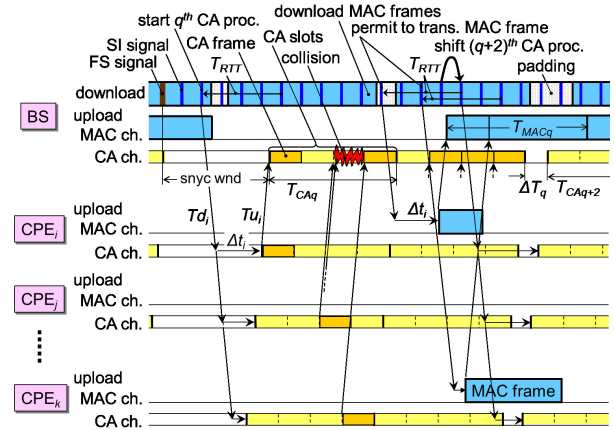


Fig. 3 An implementation of the TP system.

can run by attempting to arrive at the BS at the time of carrier extinction on the upload medium without wasting time. As a result, the throughput and the delay performances may be significantly improved and optimum performance can be achieved.

However, the introduction of OBS may cause a rapid increase in the delay due to the queue of the MAC frames, which have succeeded in the CA procedures, if it repeatedly ignores the transmission situation of MAC frames in high offered traffic. Some measures, such as flow control to the CA procedure, are necessary.

Figure 3 shows an implementation of the TP system, in which the following steps are added to the system, consisting of Steps (A) to (E) and Step (G), where Step (F) is excluded:

- (H) The upload bandwidth is divided into CA and MAC channels (“CA ch.” and “MAC ch.” on “upload” in Fig. 3), so that the average time for the CA procedure and the average transmission time of the MAC frames become almost equal in high offered traffic situations.
- (I) The BS predicts the time of carrier extinction from the T_{RTT} , the time length of the previous CA procedure, and the MAC frame length notified by CPE, and then, calculates the precedence transmission timing, which is T_{RTT} , before the time of carrier extinction (“ T_{RTT} ” in Fig. 3).
- (J) The BS proceeds independently to indicate the permission of CA frame transmission and the permission of the MAC frame transmission at the corresponding precedence transmission timing (“start q^{th} CA proc.” and “permit to trans. MAC frame” in Fig. 3).
- (K) When the MAC frames that have succeeded in the CA procedure but have not been transmitted are increasingly queued, the next-after-the-next CA procedure is delayed temporarily (“ ΔT_q ” and “shift $(q+2)^{th}$ CA proc.” in Fig. 3).

Step (H) implies that the efficiency with which the upload bandwidth is used is improved as much as possible by splitting the upload bandwidth into the CA and MAC channels that correspond to the number of CA slots during high offered traffic situations, where the upper layers generate payloads one after the other (normalized offered traffic ρ^{*3} is from 1 to 2).

Steps (I) and (J) imply that the time lost due to the intervention

*3 Total upload offered traffic, including the retry MAC frames that are unsuccessful in the CA procedure, divided by total upload bandwidth.

of RTT is eliminated by the precedence transmission of all CA and MAC frames seeking to arrive at the time of carrier extinction.

Step (J) also implies that the next $(q + 1)^{th}$ CA procedure can start without waiting for the completion of all MAC frame transmissions of the q^{th} CA procedure, although the next CA procedure starts after completing all MAC frame transmissions in the NP system, as described in Step (F).

Step (K) implies that the flow control function to restrain the increasing queue of the MAC frames by delaying the start of the CA procedure is implemented. This function is activated in cases where long MAC frames are temporarily concentrated, causing the delay to increase rapidly.

In the next section, the theoretical calculation models for the performance comparison between the NP and TP systems are discussed in detail.

3. Theoretical Calculation Models

3.1 Proper Setting of n in v-MCA

The proper setting of n based on Steps (C) and (D) is discussed in this section. The number of CA slots is set adaptively according to the offered traffic [6].

By assuming that the number of CPEs attempting the CA procedure per second does not fluctuate significantly during adjacent CA procedures, i.e., the number of CA slots n_q at the q^{th} CA procedure is almost proportional to the time interval TT_{CAq} from the $(q - 1)^{th}$ to q^{th} CA procedure, then n_q is obtained from the following recurrence relationships:

$$k_q = k_{q-1} \times \frac{TT_{CAq}}{TT_{CAq-1}} \quad (1)$$

$$n_q = \lceil k_q \rceil \quad (2)$$

where k_q is the estimated number of CPEs that attempt the q^{th} CA procedure, and $\lceil \cdot \rceil$ is the ceiling function. The validity of this assumption is evaluated later.

3.2 Maximum Throughput

3.2.1 NP System

Let $T_{INT_{RTT}}^{NP}$ be the time interval between adjacent CA procedures in the NP system with successive transmission of frames using IBS. It is given by

$$T_{INT_{RTT}}^{NP} = T_{CA_{RTT}}^{NP} + T_{MAC_{RTT}}^{NP} \quad (3)$$

where $T_{CA_{RTT}}^{NP}$ and $T_{MAC_{RTT}}^{NP}$ are " $T_{CA_{RTT}}$ " and " $T_{MAC_{RTT}}$ " in Fig. 2, respectively.

Then, the maximum theoretical throughput of the NP system is simply obtained as follows:

$$\hat{\phi}_{\max}^{NP} = \frac{T_{MAC}^{NP}}{T_{INT_{RTT}}^{NP}}. \quad (4)$$

Letting the upload bandwidth be BW^{NP} and n^{NP} be k times α^{NP} , which is the risk factor to compensate for the underestimation of k due to large fluctuations of the CA procedure intervals in IBS [6] and assuming that all CPEs that attempt the CA procedure succeed,

$$T_{CA_{RTT}}^{NP} = T_{RTT} + \frac{n^{NP} FL_{CA}}{BW^{NP}} \quad (5)$$

$$T_{MAC}^{NP} = \frac{k \cdot FL_{MAC}}{BW^{NP}} \quad (6)$$

$$T_{MAC_{RTT}}^{NP} = k \left(T_{RTT} + \frac{FL_{MAC}}{BW^{NP}} \right) \quad (7)$$

where FL_{CA} is the length of the CA slot (= CA frame length), and FL_{MAC} is the average length of the MAC frame.

Let the ratio \hat{m}^{NP} in high offered traffic situations be the ratio of the time of CA procedure and the time lost due to the intervention of RTT for the MAC frame transmission control to the transmission time of the MAC frames. Thus, the ratio \hat{m}^{NP} can be expressed as follows:

$$\hat{m}^{NP} = \frac{T_{CA_{RTT}}^{NP} + k \cdot T_{RTT}}{T_{MAC_{RTT}}^{NP}}. \quad (8)$$

Equation (4) can be rewritten using Eq. (8) as follows:

$$\hat{\phi}_{\max}^{NP} = \frac{1}{1 + \hat{m}^{NP}}. \quad (9)$$

Equation (9) implies that $\hat{\phi}_{\max}^{NP}$ is affected not only by FL_{MAC} , FL_{CA} , n^{NP} , and k but also by BW^{NP} and T_{RTT} , which depend on the upload bandwidth and network length.

3.2.2 TP System

On the other hand, the theoretical calculation model of the TP system becomes complex due to the introduction of OBS.

Let the transmission bandwidth for the CA channel be BW_{CA}^{TP} , and the transmission bandwidth for the MAC channel be BW_{MAC}^{TP} . The time T_{CA}^{TP} accommodating $n^{TP} \times$ CA slots (" T_{CAq} " in Fig. 3) is given by

$$T_{CA}^{TP} = \frac{n^{TP} FL_{CA}}{BW_{CA}^{TP}}. \quad (10)$$

The time T_{MAC}^{TP} , which is necessary to transmit all the MAC frames that are expected to succeed in the CA procedure (" T_{MACq} " in Fig. 3), is given by

$$T_{MAC}^{TP} = \frac{P_{S \max} n^{TP} FL_{MAC}}{BW_{MAC}^{TP}} \quad (11)$$

where $P_{S \max}$ (= $1/e$) is the peak of the average success probability per slot [6], [11].

The proper split-channel ratio m^{TP} , i.e., $T_{CA}^{TP} = T_{MAC}^{TP}$ in high offered traffic situations, can be expressed as follows:

$$m^{TP} = \frac{BW_{CA}^{TP}}{BW_{MAC}^{TP}} = \frac{FL_{CA}}{P_{S \max} FL_{MAC}}. \quad (12)$$

Let the expansion factor be β^{TP} , i.e., BW_{CA}^{TP} times β^{TP} , to cover the insufficiency of BW_{CA}^{TP} when CA accesses are temporarily concentrated [8]. The expanded split-channel ratio \hat{m}^{TP} is given by

$$\hat{m}^{TP} = \frac{\beta^{TP} BW_{CA}^{TP}}{BW_{MAC}^{TP} + (1 - \beta^{TP}) BW_{CA}^{TP}} \quad (13)$$

$$= \frac{\beta^{TP} m^{TP}}{1 + (1 - \beta^{TP}) m^{TP}}. \quad (14)$$

Then, the maximum theoretical throughput of the TP system is

obtained as follows:

$$\hat{\phi}_{\max}^{TP} = \frac{BW_{MAC}^{TP} + (1 - \beta^{TP})BW_{CA}^{TP}}{BW_{CA}^{TP} + BW_{MAC}^{TP}} \quad (15)$$

$$= \frac{1 + (1 - \beta^{TP})m^{TP}}{1 + m^{TP}} \quad (16)$$

$$= \frac{1}{1 + \hat{m}^{TP}}. \quad (17)$$

Further, Eqs. (10) and (11) are rewritten as follows:

$$\hat{T}_{CA}^{TP} = \frac{T_{CA}^{TP}}{\beta^{TP}} \quad (18)$$

$$\hat{T}_{MAC}^{TP} = \frac{T_{MAC}^{TP}}{1 + (1 - \beta^{TP})m^{TP}}. \quad (19)$$

Equation (17) implies that $\hat{\phi}_{\max}^{TP}$ is not a function of network length and total upload bandwidth, because m^{TP} in Eq. (12) does not depend on them. As shown in **Tables 1** and **2**, it is assumed that FL_{CA} equals 8 bytes, β^{TP} equals 1.7 and FL_{MAC} equals 355 bytes (average MAC frame length, the ratio of the numbers of short to long packets is 8 : 2). Thus, when m^{TP} and \hat{m}^{TP} are 0.0612 and 0.109, respectively, $\hat{\phi}_{\max}^{TP}$ reaches 0.902. This value is the maximum theoretical throughput in that condition for a given system.

In addition, in low traffic situations, major parts of the CA channel and MAC channel are wasted. In congested situations, such as $\rho > 2$ or more, both the CA channel and the MAC channel fall into overload.

3.3 Transmission Delay

The transmission delay is the time spent from the origination of the MAC frame in CPE to the completion of its transmission on the upload MAC channel, i.e., the delay consists of the average time taken to start the next CA procedure, the average time to achieve successful CA and the average time to complete the transmission of the MAC frame.

Table 1 Key parameters of the network for the computer simulation.

Parameters	Min.	Regular	Max.
Network topology	PTMP with tree-shaped bus		
Duplex	FDD		
Propagation speed	2/3 of light speed		
Model of packet arrivals	Table 2		
Network length	0 km	10 km	40 km
Total upload bandwidth	5 Mbps	10 Mbps	40 Mbps
Period of FS signals	51,200 bit-times		
Period of SI signals	256 bit-times		
Period of state transition	256 bit-times		
SI signal length	8 bytes		
CA frame length (FL_{CA})	8 bytes		
The number of CA slots (n)	Variable from 2 to 32 slots		
Risk factor (α^{NP})	8.0		
Expansion factor (β^{TP})	1.7		
Flow control factor (γ^{TP})	1.0		
The number of CPEs	max. 5,000		

Table 2 Key parameters for the Poisson arrival model of upload.

Parameters	Min.	Regular	Max.
MAC frame length	Short: 64 bytes, long: 1,518 bytes		
Ratio of the numbers of short to long packets	10 : 0	8 : 2	0 : 10
Average MAC frame length	64 bytes	355 bytes	1,518 bytes
Packet generation model	Poisson arrival		

3.3.1 NP System

The average delay $D_{\text{@max}}^{NP}$ around the maximum throughput can be expressed as follows:

$$D_{\text{@max}}^{NP} = \left(\frac{1}{2} + R^{NP} \right) T_{INT_{RTT}}^{NP} - \frac{1}{2} T_{MAC_{RTT}}^{NP} + T_{back-off}^{NP} \quad (20)$$

where R^{NP} is the number of CA attempts that are carried out before achieving successful CA around the maximum throughput. Let the cumulative number of CA slots after the C^{th} collision be $\mathcal{B}(C)$, which is the function with the BEB algorithm; because the average number of CA slots required for back-off at the instant of the c^{th} collision is $(2^c - 1)/2$, $\mathcal{B}(C)$ can be expressed as follows:

$$\mathcal{B}(C) = \begin{cases} \sum_{c=0}^C (2^c - 1)/2 = 2^C - C/2 - 1, & C \leq 10 \\ \mathcal{B}(10) + \frac{2^{10} - 1}{2}(C - 10), & 10 < C \leq 16. \end{cases} \quad (21)$$

where the minimum and maximum window sizes are 2 and 1,024, respectively.

Letting C be $R^{NP} - 1$, $T_{back-off}^{NP}$ is given by

$$T_{back-off}^{NP} = \frac{\mathcal{B}(R^{NP} - 1)}{n^{NP}} T_{INT_{RTT}}^{NP}, \quad (22)$$

where $\mathcal{B}(R^{NP} - 1)/n^{NP}$ is the number of CA procedures during back-off processing.

3.3.2 TP System

Because BW_{CA}^{TP} is expanded by β^{TP} times, situations such as $\hat{T}_{CA}^{TP} < \hat{T}_{MAC}^{TP}$, i.e., a time difference ΔT^{TP} between \hat{T}_{MAC}^{TP} and \hat{T}_{CA}^{TP} , may occur due to actual traffic fluctuations at every instant. MAC frames, which have succeeded in the CA procedure but have not yet been transmitted, queue one after the other, and the delay may therefore rapidly increase. If such a situation continues to occur, the effect of access dispersion by BEB processing is lost. In other words, the principle of the CBA scheme is flawed.

The flow control described in Step (K) in the CA procedure prevents the occurrence of such a situation. When the situations $\hat{T}_{CA}^{TP} < \hat{T}_{MAC}^{TP}$ continue in two or more CA procedures, starting at the next-after-the-next, i.e., the $(q + 2)^{th}$ CA procedure (“ ΔT_q ” in Fig. 3) is delayed from the following equation:

$$\Delta T_q^{TP} = \hat{T}_{MAC_q}^{TP} - \gamma^{TP} \hat{T}_{CA_q}^{TP} \quad (23)$$

where γ^{TP} is the flow control factor [8]. No flow control is activated, when $\hat{T}_{MAC_q}^{TP} \leq \gamma^{TP} \hat{T}_{CA_q}^{TP}$,

$$\Delta T_q^{TP} = 0. \quad (24)$$

Let T_{INT}^{TP} be the time interval between adjacent CA procedures including delays that are due to flow control in the TP system,

$$T_{INT}^{TP} = \hat{T}_{CA}^{TP} + \Delta T^{TP}. \quad (25)$$

Further, let $T_{back-off}^{TP}$ be the cumulative delay due to BEB processing caused by collisions in the CA procedure. Then, the average delay $D_{@max}^{TP}$ can be expressed as follows:

$$D_{@max}^{TP} = \left(\frac{1}{2} + R^{TP} \right) T_{INT}^{TP} + \frac{1}{2} \hat{T}_{MAC}^{TP} + T_{back-off}^{TP} \quad (26)$$

where R^{TP} is the number of CA attempts that are carried out before a successful CA is achieved around the maximum throughput. $T_{back-off}^{TP}$ is

$$T_{back-off}^{TP} = \frac{\mathcal{B}(R^{TP} - 1)}{n^{TP}} T_{INT}^{TP}, \quad (27)$$

Equation (20) implies that $D_{@max}^{NP}$ increases due to a longer network length but decreases due to a wider upload bandwidth. On the other hand, Eq. (26) implies that $D_{@max}^{TP}$ remains constant for a longer network length, but that it decreases due to a wider upload bandwidth, as shown in Eqs. (10) and (11).

4. Performance Evaluation

4.1 Computer Simulation Method

To evaluate the performances of the NP and TP systems, a computer simulation was performed under the network conditions shown in Table 1, which is the target range of this system, where α^{NP} , β^{TP} and γ^{TP} ^{*4} are based on the previous results [6] and [8]. Although the total upload bandwidth is up to 40 Mbps, a Giga-bit class access network can be provided by assigning a wider bandwidth to the download channel and using sector antennae for frequency re-use. The propagation speed is assumed to be $2/3^{rd}$ of the speed of light, by assuming usage of hybrid-fiber-radio and hybrid-fiber-coaxial systems. When using only radio, the propagation speed approaches the speed of light, which reduces the *RTT* and eases the design conditions of the system.

In the simulation, one BS and a maximum of 5,000 CPEs, which are located randomly in the two-dimensional network, can work together on a computer. Each machine transmits its state based on Steps (A) to (F) for the NP system and Steps (A) to (K), excluding Step (F) for the TP system at a rate of 256 bit-times, which is equivalent to the period of the SI signal sent from the BS, as shown in Table 1.

The Poisson arrival model shown in Table 2 is used in the simulation. The ratio of the number of short packets with a 64-byte length to long packets with a 1,518-byte length is different for each condition. Further, after the previous packet is sent, a new packet arrives from the upper layer according to a Poisson distribution.

In the simulation, the period of 2.5×10^7 bit-times is necessary to reach steady state. The period from 3.0×10^7 bit-times to 5.5×10^7 bit-times is defined as the measurement window Δw . Means of the simulation results during Δw were calculated. Further, to average out random fluctuations, the simulations were repeated five times with different initial values. The overall mean for each of the five runs is considered as the measured data. The standard deviation of the mean for each of the five runs is less than

^{*4} Though the appropriate value of γ^{TP} was 1.2 to improve throughput performance [8]. $\gamma^{TP} = 1.0$ is applied to maintain the stability within the target range of the system in this paper.

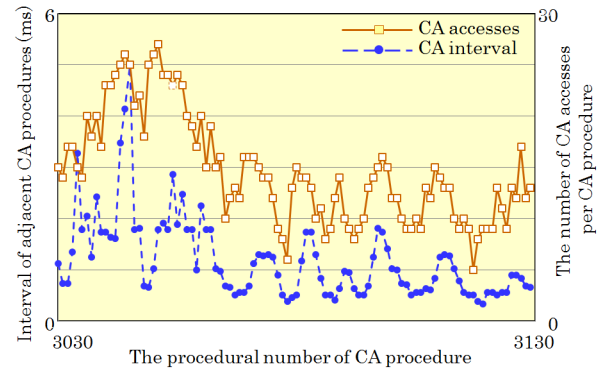


Fig. 4 Correlation between adjacent CA procedure intervals and the number of CA accesses ($\rho = 2.1$).

2% for both throughput and delay performances around $\rho = 1$.

The validity of the simulation was verified by comparing simulation results with theoretical values in specific situations, such as $\rho \ll 1$, $\rho = 1$, maximum throughput, and traffic consisting of only long packets or short packets.

4.2 Validity of Assumption on Adjacent CA Procedures

To verify the assumption that the number of CPEs attempting the CA procedure per second does not fluctuate significantly during the adjacent CA procedures in Eq. (1), the correlation between the time interval of the adjacent CA procedures and the number of CA accesses per CA procedure was evaluated, as shown in **Fig. 4**. The figure shows an example with 100 CA procedures sampled from a simulation using the regular network condition in Tables 1 and 2.

This example shows that the number of CA accesses per CA procedure follows the interval of adjacent CA procedures well, although slight time lags are observed. The correlation coefficients with 1,000 CA procedures was observed to be $r = 0.80$. This result implies that the number of CA accesses per second does not fluctuate significantly during the adjacent CA procedures, i.e., the above assumption may be adequate but its incompleteness may cause some performance degradation relative to the theoretical limit.

4.3 Performance Comparison

The values of parameters such as n^{NP} and R^{TP} are required for theoretical calculation using Eqs. (4), (20), and (26) but they cannot be obtained theoretically. Thus, the mean values calculated from simulation results were adopted. As an example, $n^{NP} = 31.6$, $n^{TP} = 25.1$, $R^{NP} = 9.4$ and $R^{TP} = 5.7$ in the regular network condition in Tables 1 and 2. Because the interval between the adjacent CA procedures in the NP system is longer than that of the TP system, R^{NP} is higher than R^{TP} . Although these parameters were different in other conditions, similar tendencies were observed.

4.3.1 Throughput and Delay versus Offered Traffic

Figure 5 shows an example of the projection of simulated results onto the theoretical performances of the NP and TP systems as a function of ρ for the above regular condition. The theoretical throughput of the NP and TP systems is calculated by

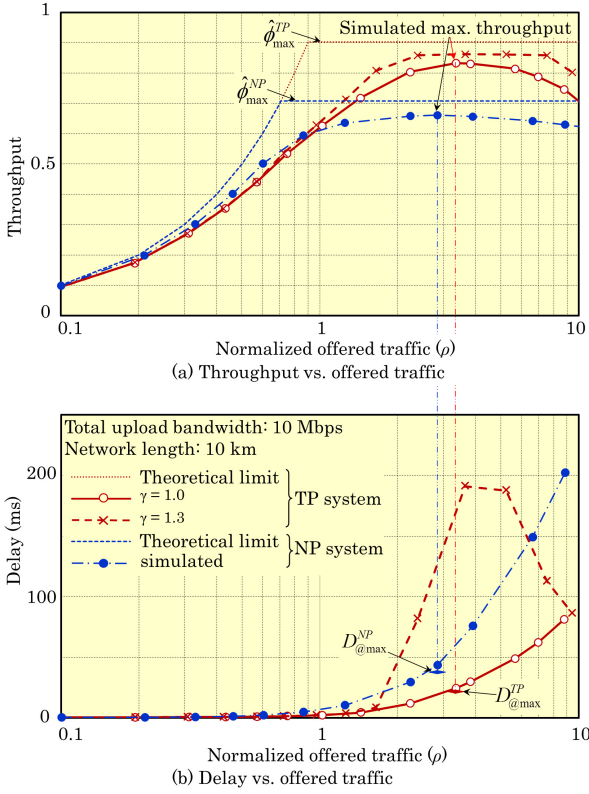


Fig. 5 An example of the performance comparison between theoretical and simulated results as a function of normalized offered traffic.

$$\hat{\phi}^{NP} = \begin{cases} \rho, & \rho < \hat{\phi}_{\max}^{NP} \\ 1/(1 + \hat{m}^{NP}), & \rho \geq \hat{\phi}_{\max}^{NP} \end{cases} \quad (28)$$

$$\hat{\phi}^{TP} = \begin{cases} \rho, & \rho < \hat{\phi}_{\max}^{TP} \\ 1/(1 + \hat{m}^{TP}), & \rho \geq \hat{\phi}_{\max}^{TP} \end{cases} \quad (29)$$

It was found that the simulated throughput of the NP system reaches its maximum at a lower ρ than that of the TP system with $\gamma = 1.0$, and that the throughput of the NP system is slightly higher than that of the TP system at $\rho < 0.9$. These are due to the greater number of CA slots being prepared in the NP system by setting $\alpha^{NP} = 8.0$ but $\beta^{TP} = 1.7$. Further, the reason that the throughput of the TP system with $\gamma = 1.3$ is higher than that with $\gamma = 1.0$, and for which the delay increases rapidly at $\rho > 1.6$, is thought to be due to the increasing queue of MAC frames, as described previously.

4.3.2 Throughput Performance

Figures 6 and 7 are projections of the maximum throughput as functions of the network length and total upload bandwidth in these samples onto the theoretical maximum throughput, while the total upload bandwidth is maintained at 10 Mbps. It was found that the NP and TP systems show the expected throughput performance. The differences between the theoretical and simulated maximum throughput are not as great as 4.5% in the NP and 7.7% in the TP systems for the regular condition in Tables 1 and 2. These discrepancies are believed to be due to the quantization errors of the SI signal sent periodically with a period of 256 bit-times, and time lags between CA intervals and CA accesses due to the incomplete assumption on adjacent CA procedures as described above. In addition, the effect of the flow control can not be ignored in the TP system, because the difference decreases

from 7.7% to 4.6% by setting $\gamma^{TP} = 1.1$ to restrain flow control activations around the maximum throughput.

As expected, high throughput performance regardless of network length and total upload bandwidth is confirmed in the TP system. Further, the maximum throughput of the TP system is 26% to 118% higher than that of the NP system for 10–40 km and 10–40 Mbps, respectively. However, the NP system shows a slightly higher maximum throughput for a range of 2.5 km or less, because the overhead, which cannot be overlooked, remains constant in the CA procedure of the TP system by introducing OBS.

Figure 8 shows the performance comparisons of the theoretical and simulated maximum throughputs for various average MAC frame lengths, i.e., for ratios of the number of short to long packets that range from 10 : 0 to 0 : 10, while the network length and the upload bandwidth are maintained at 10 km and 10 Mbps, respectively. Saturation curve characteristics due to longer average MAC frame lengths are observed in both the NP and TP systems. However, the differences between the theoretical and simulated maximum throughput increase due to shorter MAC frame lengths, such as 12.4% (15.1% when setting $\gamma^{TP} = 0.9$ as discussed later) in the TP system and 9.0% in the NP system for a ratio of 10 : 0. This discrepancy is thought to be caused by the quantization error of the SI signal, because the average error, i.e., the half of the SI interval is 128 bit-times, and its percentage of transmission bit-times of MAC frame increases due to shorter MAC frame lengths, such as 1.1% at 0 : 10, 4.5% at 8 : 2 and 25.0% at 10 : 0.

4.3.3 Delay Performance

Figure 9 shows the projection of the delay around the maximum throughput ($\rho \approx 3$) as a function of the network length. It was confirmed that the delay of the TP system is almost constant in both theoretical and simulated results, although the simulated results are about 12% higher than the theoretical results. The NP system increases due to longer network length, although the simulated results are about 20% higher than the theoretical results. As indicated by $n^{NP} = 31.6$, which was described above, this is believed to be affected by the number of CA accesses that often exceed the proper number of accesses for the upper limit of the number of CA slots, which is defined as 32 in Table 1. Further, at 10 km, the percentages of ΔT^{TP} and $T_{back-off}^{TP}$ are about 6% and 10% of D_{\max}^{TP} , respectively, while $T_{back-off}^{NP}$ is about 54% of D_{\max}^{NP} . When considering the rapid increases of the delay around the maximum throughput, it can be said that Eqs. (20) and (26) provide good estimations.

Figure 10 shows the projection as a function of the total upload bandwidth. It is found that the delay of both the NP and TP systems decreases due to the wider total upload bandwidth, although the NP system is twice as large as the TP system.

Figure 11 shows the projection as a function of the average MAC frame length. It was found that the delay of both the NP and TP systems increases almost linearly due to the longer MAC frame length, as shown in Eqs. (7) and (11). However, the difference between the theoretical and simulated delay increases slightly due to the shorter MAC frame length in the TP system. This is believed to be caused by the increasing queue of the MAC frames that are to be transmitted due to the shorter MAC frame

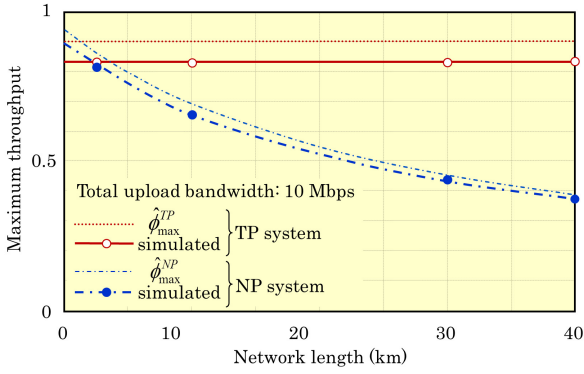


Fig. 6 Performance comparison between theoretical and simulated maximum throughput as a function of the network length.

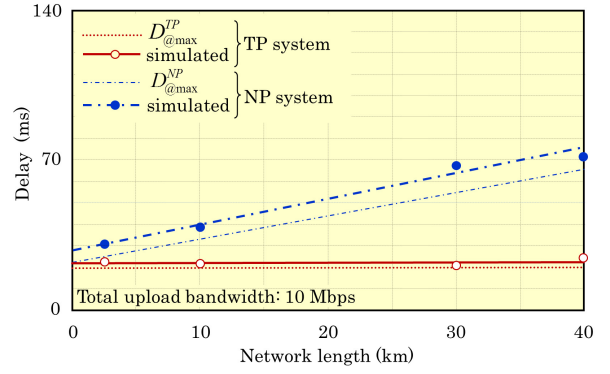


Fig. 9 Performance comparison between theoretical and simulated delays at maximum throughput as a function of the network length.

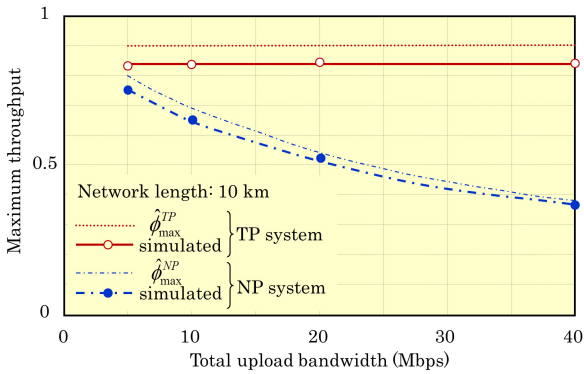


Fig. 7 Performance comparison between theoretical and simulated maximum throughput as a function of the total upload bandwidth.

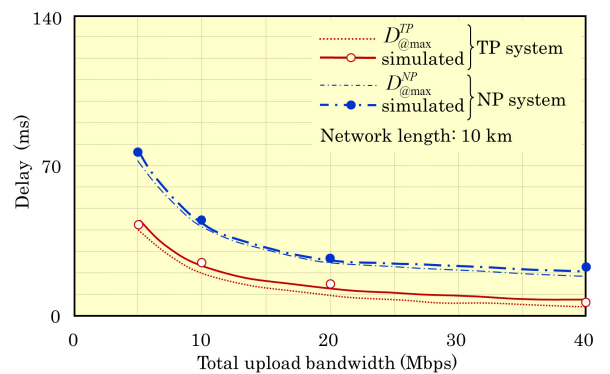


Fig. 10 Performance comparison between theoretical and simulated delays at maximum throughput as a function of the total upload bandwidth.

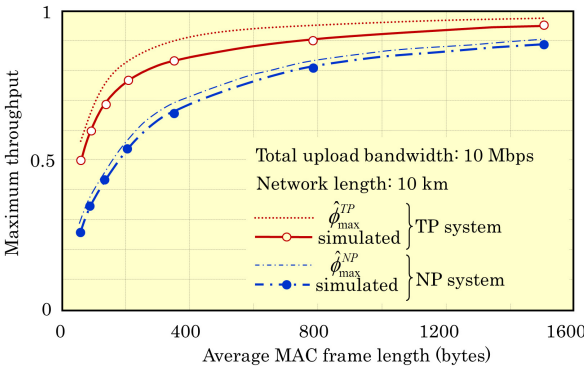


Fig. 8 Performance comparison between theoretical and simulated maximum throughput as a function of the average MAC frame length.

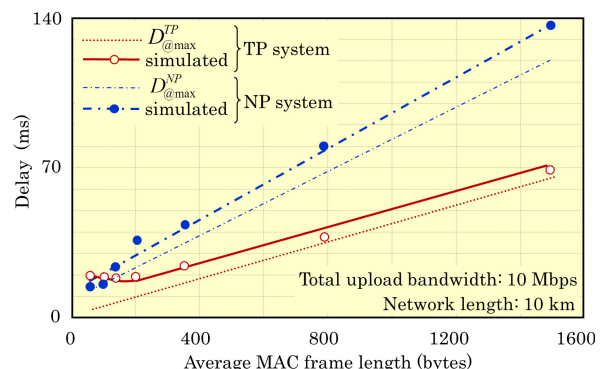


Fig. 11 Performance comparison between theoretical and simulated delays at maximum throughput as a function of the average MAC frame length.

length, while the flow control is not often activated. This is because the difference decreases from 20.7 ms to 8.4 ms at the ratio of 10 : 0 by setting $\gamma^{TP} = 0.9$ to enhance flow control activations.

Thus, it can be concluded that the TP system maintains good delay performance relative to the NP system.

5. Conclusions

After discussing the MAC mechanisms and the theoretical calculation models of the synchronous v-MCA adopted to the NP and TP systems, their system performances were evaluated by comparing theoretical and simulated results. Based on the results, the followings points were confirmed:

(1) There were time lags due to the quantization error of the SI signals and due to the incomplete assumption regarding adjacent CA procedures. In addition, the flow control in the TP

- system caused slight differences between the theoretical and simulated results. However, the theoretical calculation models provided a good approximation of the maximum throughput and delay performances in both the NP and TP systems.
- (2) The TP system provides an ideal maximum throughput performance regardless of the network length and total upload bandwidth, while maintaining the low delay characteristics of a CBA scheme.
- (3) The maximum throughput of both the NP and TP systems shows saturation curve characteristics that are due to the longer MAC frame length, but their delay increased linearly.
- (4) Because there is a constant overhead in the CA procedure of the TP system due to the introduction of OBS, the NP system shows a slightly higher maximum throughput in the range of

2.5 km or less when the total upload bandwidth is 10 Mbps.

- (5) Although the delay performance of the TP system is almost constant for a given network length, it decreases when there is a wider upload bandwidth, and it increases linearly for a longer average MAC frame length, but it is half or less of that of the NP system.

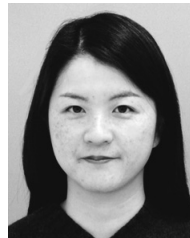
Because \hat{m}^{TP} depends on the average MAC frame length, the BS may maintain the network in its best condition by monitoring incoming traffic and adaptively controlling the split-channel ratio of CA and MAC channels using multiplexing techniques such as OFDM. Furthermore, we intend to study whether synchronous v-MCA with the TP scheme can achieve significant performance improvements over wireless LANs in the unlicensed spectrum sharing environment.

References

- [1] Data-over-cable service interface specifications, cable modem termination system network side interface specification, MCNS Consortium (1996).
- [2] IEEE Std 802.16-2004, Air interface for fixed broadband wireless access systems (2004).
- [3] Data-over-Cable Service Interface Specifications (DOCSIS), Understanding Data Throughput in a DOCSIS World, CISCO Systems (2008).
- [4] Kobayashi, H., Ozawa, K., Kamura, K. and Moriya, O.: Synchronous CSMA/CD on PTMP access networks, *IEICE Trans.*, Vol.85-B, No.4, pp.471–479 (2002).
- [5] Moriya, O. and Kobayashi, H.: Colliding probability reduction by synchronous carrier sense multiple access with multiple collision avoidance for point to multipoint access networks, *IPJS Journal*, Vol.44, No.3, pp.932–941 (2003).
- [6] Moriya, O. and Kobayashi, H.: Variable collision avoidance slots for synchronous CSMA/MCA system on PTMP access networks, *IPJS Journal*, Vol.44, No.8, pp.2208–2217 (2003).
- [7] Moriya, O., Mori, Y., Takahashi, T. and Kobayashi, H.: Precedence transmission of frames incorporating synchronous CSMA/v-MCA on PTMP access networks, *IPJS Journal*, Vol.48, No.4, pp.1758–1766 (2007).
- [8] Sano, K., Moriya, O., Matsunaga, S., Uneno, Y. and Kobayashi, H.: Total precedence transmission of frames incorporating synchronous CSMA/v-MCA on PTMP access networks, *IEICE Trans.*, Vol.93-B, No.8, pp.1075–1086 (2010).
- [9] Sano, K., Kobayashi, H. and Moriya, O.: An advanced CSMA/CA system for wide area broadband wireless access, *Proc. IEEE ICC 2011* (2011).
- [10] IEEE Std 802.3, 2000 Edition, Part 3: Carrier sense multiple access with collision detection (CSMA/CD) access method and physical layer specifications (2000).
- [11] Kleinrock, L. and Tobagi, F.A.: Packet switching in radio channels: Part I - Carrier sense multiple-access modes and their throughput-delay characteristics, *IEEE Trans. Commun.*, Vol.COM-23, No.12, pp.1400–1416 (1975).
- [12] Tantra, J.W., Foh, C.H., Tinnirello, I. and Bianchi, G.: Out-of-band signaling scheme for high speed wireless LANs, *IEEE Trans. Commun.*, Vol.6, No.9, pp.3256–3267 (2007).
- [13] Tobagi, F.A. and Kleinrock, L.: Packet switching in radio channels: Part III - Polling and (dynamic) split-channel reservation multiple access, *IEEE Trans. Commun.*, Vol.COM-24, No.8, pp.832–845 (1976).
- [14] IEEE Std 802.11, 2007 Edition, Wireless LAN medium access control and physical layer specifications (2007).
- [15] Deng, J., Han, Y.S. and Hass, Z.J.: Analyzing split channel medium access control schemes, *IEEE Trans. Wireless Commun.*, Vol.5, No.5, pp.967–971 (2006).
- [16] Yang, X., Vaidya, N.H. and Ravichandran, P.: Split-channel pipelined packet scheduling for wireless networks, *IEEE Trans. Mobile Computing*, Vol.5, No.3, pp.240–257 (2006).



Hiroshi Kobayashi received his B.E. and Dr.Eng. degrees from Tokyo Institute of Technology in 1970 and 1987, respectively. He worked at Toshiba from 1970 to 2002. He is a professor at joined School of Information Environment at Tokyo Denki University in 2002. His current research interests are broadband networks, measures against cyber-attack, educational technology and measures against Internet addiction.



Kaoru Sano received her B.E. degree from Osaka University in 1993, and Dr.Eng. degree from Tokyo Denki University in 2010. In 1993, she joined Kobe Steel, Ltd. Currently, she is an adjunct lecturer in School of Information Environment at Tokyo Denki University. Her research interests are wide area broadband wireless networks and learning support systems to enhance student's motivation. She is a member of IEICE.



Osamu Moriya received his B.S. degree in Electrical Engineering from Waseda University in 1990, and M.S. degree in Electrical and Engineering from the University of Tokyo in 1992. In 1992, he joined Toshiba, Ltd. He is involved in researches on wireless communication systems, mobile security systems, and microwave semiconductors. He is a member of IEICE.